

EMULSION FORMATION IN A T-JUNCTION MICROFLUIDIC DEVICE WITH ELLIPTIC CROSS SECTION

Deibi E. García Campos, deibi20979@hotmail.com

Márcio da Silveira Carvalho, mse@puc-rio.br

PUC-Rio, Department of Mechanical Engineering, Rua Marques de São Vicente 225, Gávea, 22453-900 Rio de Janeiro, RJ, Brazil

Abstract. *The two phase oil-water flow inside reservoirs can lead to emulsion formation. The ability to predict the occurrence of emulsions and its morphological characteristics is crucial for predictions of pressure loss along well and risers and the optimization of the phase separations processes. The mechanisms responsible for emulsion formation are directly related to the two phase flow in the pore scale. Here, we use a T-junction microfluidic device as a model for the connection between two pore throats to study the emulsion formation and its characteristics as a function of liquid properties and flow rates. This geometry is extensively used in the literature to study emulsion formation, since it leads to mono dispersed emulsions, which are critical in many applications. We show the effect of the elliptic cross section of the channel on the drop size, propose a new correlation that better describes our experimental results, and prove that the transition between the different flow regime is not only a function of the continuous phase capillary number, as suggested in the literature.*

Keywords: *T-junction, droplets, microcapillary, squeezing, emulsions.*

1. INTRODUCTION

The two phase flow of oil and water inside oil reservoirs may lead to the formation of emulsions, which may cause different problems during oil production, such as changes in the flow pattern in the porous media, changes in the pressure loss in the flow along wells and risers and difficulties on the separation of both phases, as discussed by Kokal (2005) and Raikar *et al.*, (2009).

The fundamental understanding of the mechanisms responsible for emulsion formation and the characteristic of the emulsions formed as a function of operating parameters and liquid properties are still not available.

The mechanisms of emulsion formation in porous media is directly related to the two phase oil-water flow in the pore scale, how the phases arrange themselves in a continuous and dispersed phase, and how the dispersed phase breaks into small droplets. Therefore, the fundamental understanding of emulsion formation in porous media can be built by understanding the two-phase flow through micro channels.

In this work, we experimentally study the oil-water flow through a T-shaped microfluidic junction, which represent a model of a particular configuration of pore throats inside a porous material. The main goal is to determine the drop size of the dispersed phase as a function of the flow rate of each phase, liquid properties and geometry of the channels.

This flow has been extensively explored in the literature since it leads to the formation of emulsions with drops of the same size that can be easily controlled by the flow rates of each phase (Thorsen *et al.*, 2001, Nisisako *et al.*, 2005, Garstecki *et al.*, 2006 and others). The production of mono dispersed emulsion is crucial in many applications, such as medical, pharmaceutical and biological (Tice *et al.*, 2003), crystallization of proteins (Zheng *et al.*, 2004) and synthesis of nanoparticles (Gunther *et al.*, 2004), and others.

The flow in microchannels is characterized by low Reynolds number ($Re = \rho_c u_c D / \mu_c \ll 1$, with ρ_c , u_c and μ_c being the density, average velocity and viscosity of the continuous phase respectively, and D the characteristic width of the main channel), which indicates that viscous forces are stronger than inertial forces. The main force balance is between viscous and capillary forces, that define the capillary number. Most of the work in the literature is focused on characterization, and preferably developing a scaling law, of the drop size for the different flow regimes (Garstecki *et al.*, 2006, Xu *et al.*, 2006 and 2008, Fu *et al.*, 2010). They used microfluidic T-junction with rectangular cross-sections. The formation mechanisms of droplets can be divided into three mechanisms, which are defined as a function of the capillary number of the continuous phase. Here, we analyze the drop formation in a T-junction microfluidic device with an elliptic cross section at different oil and water flow rates and viscosity ratio. We show the effect of the channel cross section on the drop size, propose a new correlation that better describes our experimental results, and prove that the transition between the different flow regime is not only a function of the continuous phase capillary number, as suggested in the literature.

2. EXPERIMENTAL SETUP

2.1. Geometry features of the T-junction

The T-junction is formed by two inputs and one output channels. In our case we call the main channel, the one that carries the continuous phase and the emulsion formed, and the secondary channel, the one that carries the fluid that forms the dispersed phase. The dimensions of the T-junction used are shown in Fig. 1:

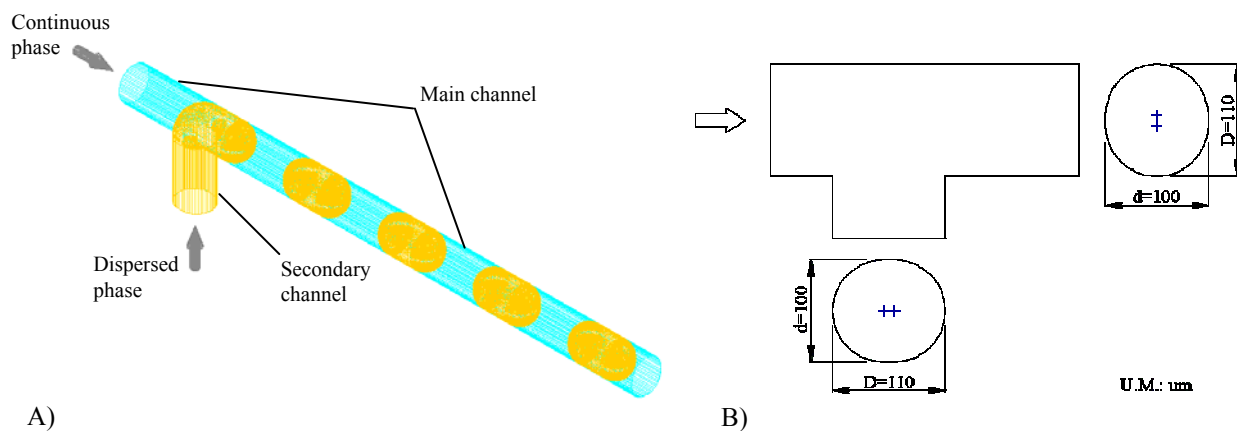


Figure 1. A) A Schematic illustration of the microfluidic T-junction with channels of elliptic cross section when two immiscible liquids are injected. B) Detail of the dimensions of the microfluidic T-junction.

The cross section of main channel is elliptic and is equal to the cross section of secondary channel, therefore we have only one geometric parameter which characterizes our geometry, that is the constant cross section of the main channel. The geometry of the cross section has a strong influence on the flow. In a rectangular cross section, the dispersed phase does not occupy the corners of the cross section, because it would require very high pressures to form an interface with a small radius of curvature. Therefore, the continuous phase flows through this area. In an elliptic cross section, the continuous phase can only flow through the thin film between the drop and the wall, as shown in Fig. 2.

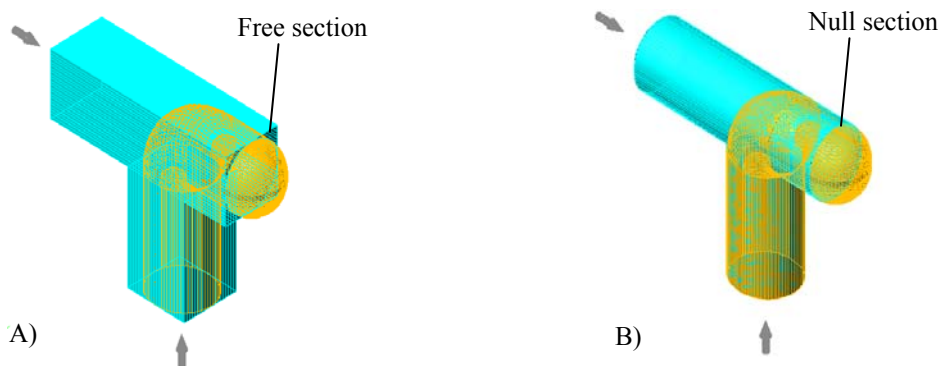


Figure 2. A) T-Junction with rectangular section, the spherical form of the interface of the emerging drop leaves a free section that allows a flow of the continuous phase. B) T-Junction with elliptic section, the interface of the drop adopts the form of the cross section leaving practically null the free section for the continuous phase.

2.2. Injected fluids:

In order to be able to determine the effect of the viscosity ratio in the behavior of droplet formation, we used two different oils as dispersed phase, as indicated in Tab. 1. As continuous phase, we used water with surfactant. The surfactant was used in order to maintain the stability of the emulsion formed. In all cases the fluids were filtered through of a mesh of 0.2 μm .

2.3. Equipments

Both fluids were injected into the microfluidic device using syringe pumps (Cole Parmer). For the continuous phase, we used syringe pumps model 780100C, with a minimum injection of 0.01 ml/hr, and the model 780200C for injection of the dispersed phase with a minimum injection of 0.001 ml/hr. The pumps contain a microprocessor that controls a stepper motor and gears, which allows to control the injected flow with 0.5% accuracy and reproducibility of 0.2%.

All experiments were made using Hamilton Gastight syringes, Series 1000. The syringes body is made of borosilicate glass and the plunger is made of PTFE coated aluminium and equipped with a precision PTFE seal. The flexibility of the seal allows the interchange of glass barrel and plunger between syringes of the same capacity. All parts in contact with the samples are made of inert materials such as glass and PTFE. The dimensional stability of the parts doesn't allow leakage of fluid or gas at high pressures (up to 200 psi).

The connections between the syringes and microcapillary system that contains the T junction were designed to contain the minimum quantity of elements, the minimum volume to accelerate the effect of the bombs in the formation of droplets, and to be the most rigid possible to minimize the risk of leaks and volume changes.

Table 1. Properties of the injected liquids

Liquids's Properties	Dispersed phases		Continuous phase
	Oil Talpa 30	Oil Velocite N°6	Water + Surfactant ⁽²⁾
Viscosity (mPa.s) ⁽¹⁾	438.13	16.90	0.97
Interfacial tension (mN/m) ⁽¹⁾	3.16	0.77	---
Density (g/mL) ⁽¹⁾	0.9086	0.8537	0.9987

⁽¹⁾: Measured at 23°C

⁽²⁾: Sodium dodecyl sulfate (2 CMC \approx 2,3 g/L of water)

2.4. Image Analysis

We used an inverted optical microscope Axiovert 40MAT (Carl Zeiss) operated with transmitted light, to visualize the behavior of the formation of droplets in the microfluidic T junction. The microscope has five objectives (2.5x, 5x, 10x, 20x and 50x) and is adapted directly with a special camera PixelINK PL-A662 for applications of microscopy. The camera transmits images in real time to the computer allowing its visualization on the monitor. The analysis of the images was performed using the AxioVision 4.7 software also from Carl Zeiss. This software allows the acquisition and processing of images and videos and has tools for manual and automatic measurements of parameters such as distances, diameters and areas, among others.

2.5. Experimental Procedure

First, the microfluidic device was filled with water, the wetting phase. The water syringe was connected to the main channel and the oil syringe to the secondary channel. In order to cover a wide range of capillary number, the water flow rate varied from 0.01 ml/h to 0.15 ml/h. At each water flow rate, the oil flow rate (dispersed phase) varied from 0.001 ml/h to 0.13 ml/h (higher oil viscosity) and 0.19 ml/h (lower oil viscosity). The range of flow rate of each phase was limited by the ability of each pump to deliver the desired flux and by the pressure distribution at the point where the two channels met. The image of the area where the drops are formed was recorded only after the stabilization of the system, which took only a few minutes at high flow rates but up to two hours at lower end of the range explored.

2.6. Models of droplets formation in the T-junction.

Garstecki *et al.* (2006) studied the formation of droplets in a microfluidic T junction of rectangular cross section, determining that, at low capillary numbers, the breakup isn't dominated by shear stresses as suggested by Thorsen *et al.*, 2001. Their experimental results showed that the dominant contribution is the pressure differential generated around the emerging droplet. He proposed a simple scaling model that predicts the droplet size formed in a microfluidic T junction of rectangular cross section. The breakup mechanism is divided in two main steps. First, the dispersed phase, from the secondary channel, enters and blocks the main channel. At this point the droplet size is approximately equal to the width of channel w . Then the increased pressure in the continuous phase upstream on the liquid-liquid interface starts to "squeeze" the neck (of characteristic width d) of the emerging droplet. The thickness of the neck decreases at rate which is approximately equal to the average velocity of the continuous phase $u_{squeeze} \approx u = Q_c/hw$. During this process the droplet grows at rate $u_{growth} \approx Q_d/hw$. The final droplet size is $L \approx w + (d/u_{squeeze})u_{growth} = w + dQ_d/Q_c$, or in form dimensionless $L/w = 1 + \alpha(Q_d/Q_c)$, with $\alpha = (d/w)$. Garstecki considers $\alpha = 1$ among other reasons because part of the continuous phase goes around the droplet and it doesn't contribute to the squeeze, and because the speed at which the neck breaks is not constant.

De Menech *et al.* (2008) identified three regimes of droplet formation in a microfluidic T junction of rectangular cross section: squeezing, dripping and jetting. The squeezing regime (low Ca), is the regime described by Garstecki *et al.* (2006). The numeric results of De Menech showed that the time to squeeze the neck ($t_{squeeze}$) of the emerging droplet is independent of Ca , while the time to block the main channel (t_{block}) grows as Ca decreases. This result confirms the intuitive fact that $t_{squeeze}$ depends only on the velocity of the outer fluid, which is responsible for the buildup of the

pressure that is required to compress the neck, whose displacement will progress at a rate proportional to the flux of the dispersed phase.

The dripping regime is preceded by a transition regime from low to high Ca . In this case, the dispersed phase enters into the main channel, but it does not blocked it completely, and the breakup point moves downstream of the T-junction, dragged by the shear stress of the continuous phase. The dripping regime has a greater influence of viscous effects. The scalar models proposed by Umbanhowar *et al.* (2000) and Thorsen *et al.* (2001) establish that breakup occurs when the interfacial force is balanced by the shear force, such that $r \sim \sigma / (\mu \varepsilon)$, where r is the final droplet radius and ε is the shear rate exerted on the droplet, based upon the average velocity of flow of the continuous phase. During the process, the emerging droplet reduces the cross section of the main channel that contains the continuous phase (Thorsen *et al.*, 2001). To keep the ratio of injected flow, the flow of the continuous phase accelerates through the free space between the emerging droplet and the wall of the main channel, exerting a larger shear stress on the droplet interface. This effect results in the formation of smaller droplets than those formed in the case where the channel is blocked completely (De Menec *et al.*, 2008).

The jetting regime occurs only at high continuous phase flow rates, low interfacial tension, i.e. at high values of capillary number. In this case the breakup point moves progressively downstream in each cycle and a jet is formed. This is a transition from the stable dripping regime to a jetting regime. This regime hasn't been explored in detail (De Menec *et al.*, 2008).

Christopher *et al.* (2008) studied experimentally the transition from squeezing to dripping regime in T-shaped microfluidic junctions of rectangular cross section. The capillary number and flow rate ratio were varied over a wide range for different viscosity ratios and different ratios of the inlet channel widths. The range corresponds to the region in which both the squeezing pressure is high when the emerging interface obstructs the channel, and the viscous shear stress on the emerging interface strongly influence the process. In this regime, the droplet size depends on the capillary number, the flow rate ratio, and the ratio of inlet channel widths, which controls the degree of confinement of the droplets. The viscosity ratio influences the droplet size only when the viscosities are similar. When there is a large viscosity contrast in which the dispersed-phase liquid is at least 50 times smaller than the continuous-phase liquid, the resulting size is independent of the viscosity ratio and no transition to a purely squeezing regime appears. In this case, both the droplet size and the droplet production frequency obey a power-law behavior with the capillary number, consistent with expectations based on mass conservation of the dispersed-phase liquid. Scaling arguments are presented that result in predicted droplet volumes that depend on the capillary number, flow rate ratio, and width ratio in a qualitatively similar way to that observed in experiments.

3. RESULTS

3.1. Proposed Model for drop size in the squeezing regime

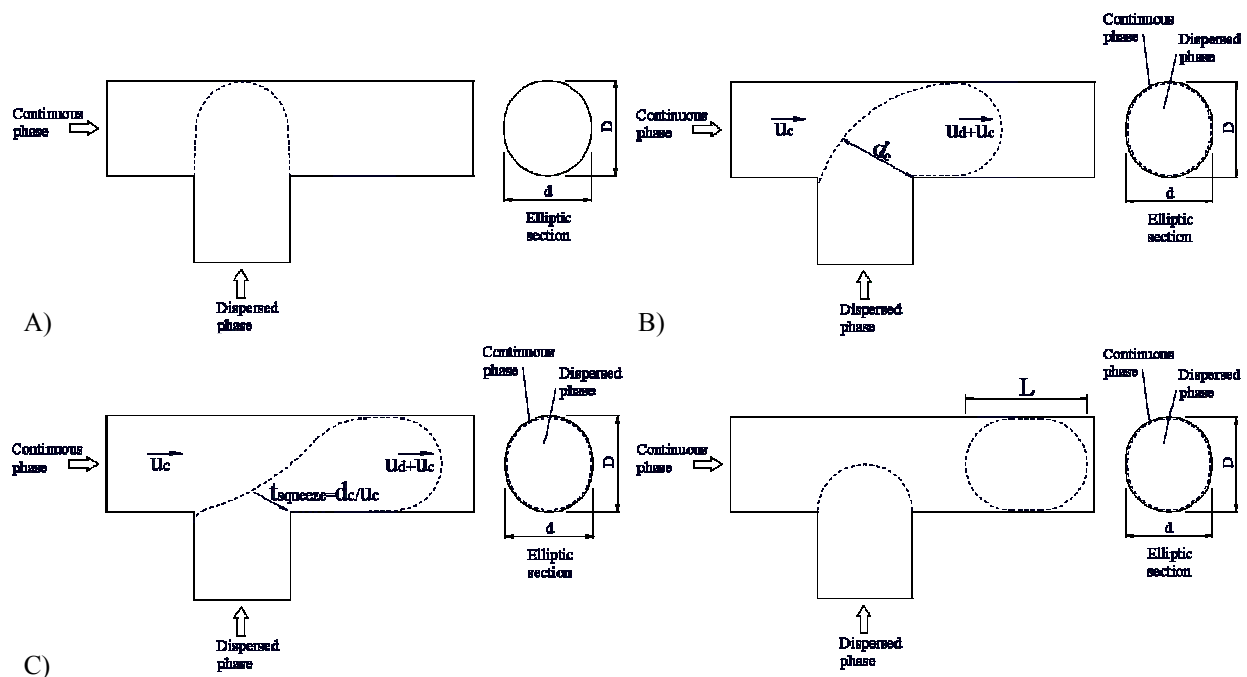


Figure 3. A) The dispersed phase blocks the channel, the drop size is D . B) The drop grows downstream to reason of $u_{growth} \approx u_d + u_c = (Q_d + Q_c) / A_{section}$. C) The neck d_c decreases to reason of $u_{squeeze} \approx Q_c / A_{section}$. When the neck breaks, the drop size is $L \approx D + (d_c / u_{squeeze}) * (u_{growth}) = D + d_c * (Q_d / Q_c + 1)$, or dimensionless $L/D = 1 + \alpha(Q_d / Q_c + 1)$.

Following the model of breakup in a microfluidic T junction of rectangular cross section (Garstecki *et al.*, 2006), we consider an alternative model to predict the droplet size formed in a microfluidic T junction with an elliptic cross section. The main difference is that since the cross section does not have corners, the continuous phase can only flow relative to the droplet through the thin film formed between the drop and the channel wall. Therefore, the average velocity of the tip of the drop is not simply u_d , as proposed by Garstecki *et al.* (2006), but the sum of $u_d + u_c$, as indicated in Fig. 3.

The growth of the droplet downstream of the T junction is related to rise by the pressure upstream and the continued injection of the dispersed phase. During this process the droplet grows at rate $u_{growth} \approx u_d + u_c = (Q_d + Q_c) / A_{section}$. The increased pressure in the flow of the continuous phase, upstream of the emerging droplet is generated when the dispersed phase blocks the main channel. During this step also is produced the thinning of the neck (d_c) of the emerging droplet in the junction. The thickness of the neck decreases at rate that is approximately equal to the average velocity of the continuous phase $u_{squeeze} \approx Q_c / A_{section}$. The stage ends when the neck breaks. A third stage occurs when part of the neck after the breaks is removed to the dispersed phase in the secondary channel and then a new cycle starts. At the end, the droplet size is $L \approx D + (d_c / u_{squeeze})(u_{growth}) = D + d_c(Q_d / Q_c + 1)$, or in dimensionless form: $L/D = 1 + \alpha(Q_d / Q_c + 1)$ with $\alpha = (d_c / D)$.

The process is repetitive and uniform in stable conditions. Thus the droplet size can be adjusted according to the rate of flow of the liquids injected (continuous and dispersed phase).

Measurements of the velocity of the tip of the drop, presented in Fig. 4, show that our hypothesis on the growth rate of the drop is valid.

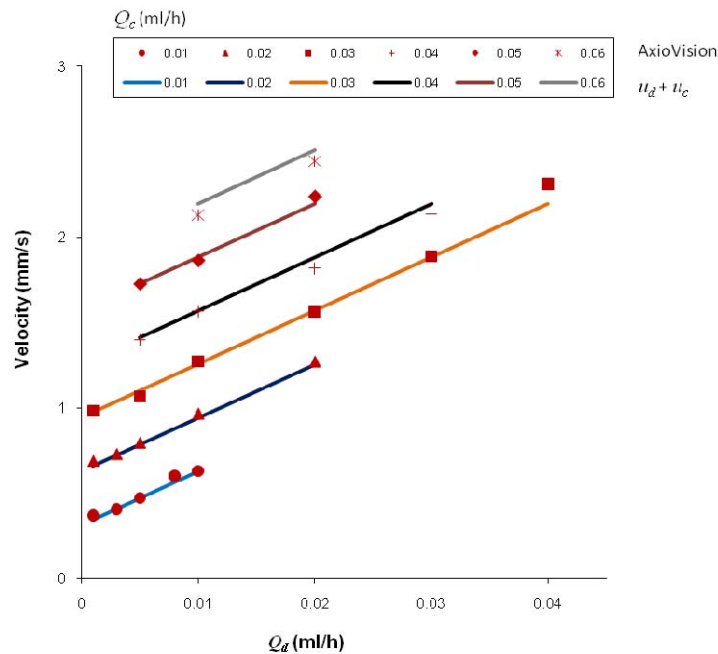


Figure 4. Comparison of the drop velocities after the junction. Measures (by AxioVision software) and the calculated (by the sum of the average velocities of the phases before from the junction $u_d + u_c$)

3.2. Measured drop size

The first set of experiments were performed with the oil with a viscosity $\mu = 438$ cP. The length of the formed drop as a function of flow rate ratio at different flow rates of the continuous phase is shown in Fig.5. The plot also shows curves that correspond to the scale model proposed by Garstecki *et al.*, (2006) – dotted line – and the model we propose in this work – continuous line. At low continuous phase flow rate ($Q_c \leq 0.03$ ml/h), the drop size is only a function of the flow rate ratio. Images of the break up process clearly show the squeezing mechanism, as discussed in the literature. At high continuous phase flow rate, $Q_c > 0.03$ ml/h, the three mechanisms can be observed. At low flow rate ratios, the squeezing mechanism is present. The proposed model for squeezing describes well how the drop size varies with flow rate ratio. The model for rectangular cross section (dotted line) under predicts the drop size. At intermediate flow rate ratio, the neck is pushed downstream by the viscous drag of the continuous phase and drops are formed by the dripping phenomenon. At high flow rate ratio, the break up point moves downstream and drops are formed by the breakup of a liquid jet, in what was called by De Menech *et al.*, (2008) jetting. Inserts in the plot show the flow configuration at these

different regimes. It is important to notice that for the system analyzed here, the transition is not a function of the capillary number alone, as discussed in the literature. At the same capillary number (continuous phase flow rate), the three regimes could be observed as the dispersed flow rate varied.

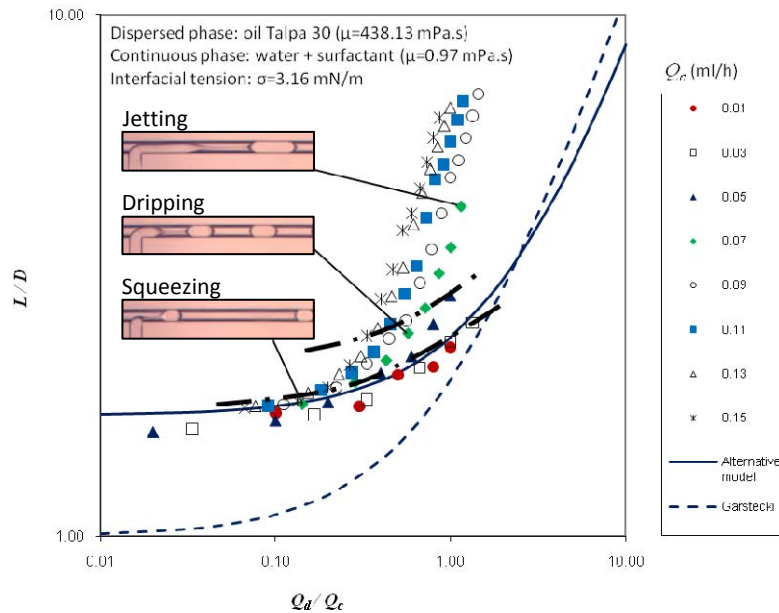


Figure 5. System with high viscosity ratio and observed regimes of formation of drops (the dash dot lines divide the regions where the regimes were observed). The patterns are shown for rectangular sections (Garstecki), and for elliptic sections (our alternative model). The model is good for to describe the squeezing regime.

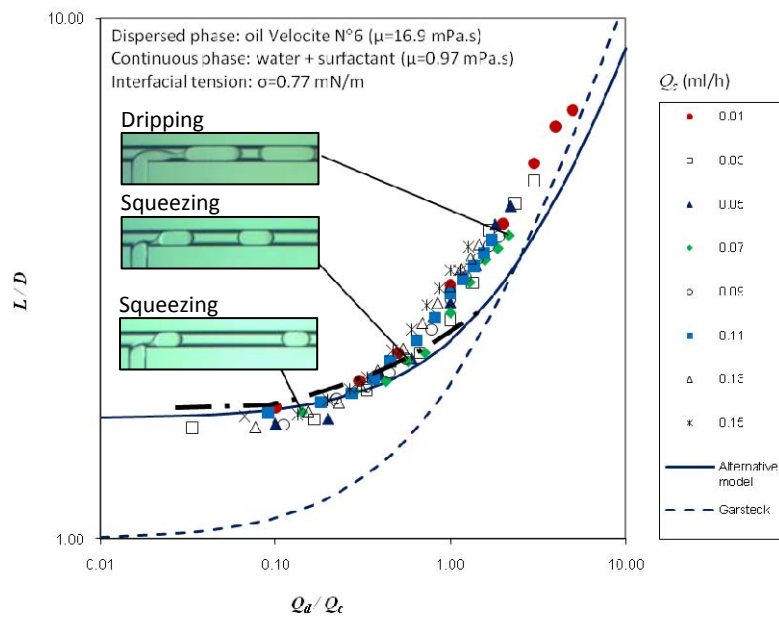


Figure 6. System with low viscosity ratio and observed regimes of formation of drops. The patterns are shown for rectangular sections (Garstecki), and for elliptic sections (our alternative model). The dash dot line divides the region where the model predicts well the droplet size. Outside of the region, the three regimes were observed.

The effect of the viscosity ratio was probed by running the same experiments with a lower viscosity oil ($\mu = 17$ cP). Unlike the high viscosity ratio, the drop size is only a function of the flow rate ratio. Curves at different continuous phase flow rate lay to top of each other, as indicated in Fig.6. The squeezing regime is clear up to a flow rate ratio of approximately 1. Above this value, the drop neck is pushed downstream by the viscous drag, characterizing the dripping phenomenon.

At high enough flow rate ratios, the drops obtained with the lower viscosity oil are consistently smaller than those obtained with the high viscosity model. Lower viscosity drops are easier to deform, leading to faster break ups.

Figure 7 shows the results for both oils plotted as a function of the capillary number for three different values of the dispersed phase flow rate. It is important to notice that at a fixed value of capillary number, we can observe different breakup regimes, a different behavior than reported in the literature. One possible reason is the viscosity ratio. In our analysis, the dispersed phase is more viscous than the continuous phase. In the analyses presented in the literature, the dispersed phase was always less viscous than the continuous phase. The effect of the capillary number on the drop size is a strong function of the dispersed phase flow rate. At low oil flow rate, the drops are formed by the squeezing mechanism and the effect of the capillary number is very weak. At high oil flow rate, drops are formed by the dripping (lower oil viscosity) or jetting (higher oil viscosity) and the drop size falls as the capillary number rises. The results are well described by a power-law relation: $L/D \sim Ca^{-0.2}$.

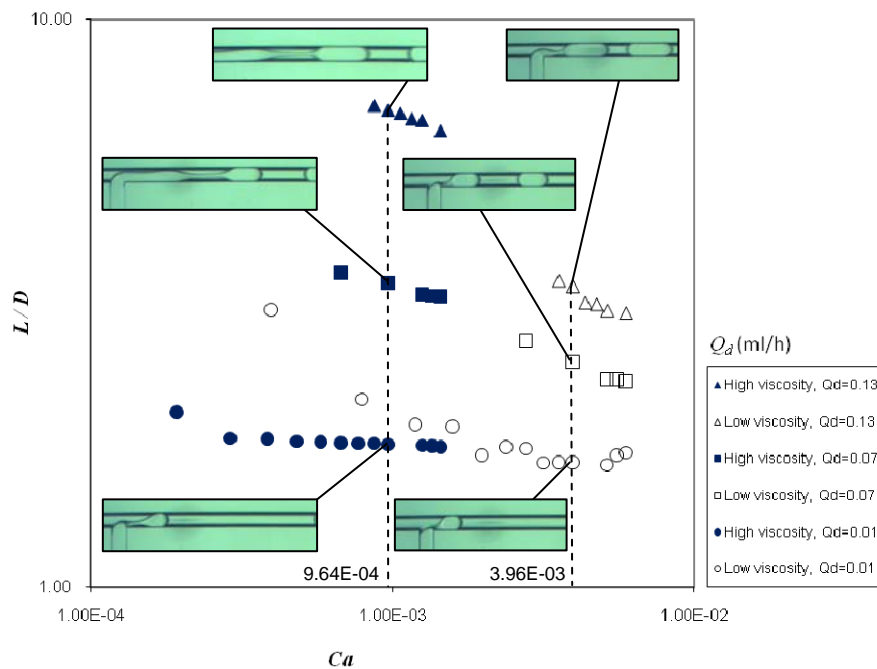


Figure 7. Influence of the capillary number on the drop size. Different regimes of formation of drops are observed for the same Ca (when $Q_c = 0.1$ ml/h). In all the cases the L/D decreases when Ca increases. At low flow of dispersed phase ($Q_d = 0.01$ ml/h), the effect of the capillary number is very weak.

4. CONCLUSION

This paper presents an experimental analysis of the formation of mono dispersed oil-water emulsions in a T-junction microfluidic device with an elliptic cross section. In our experiments, the dispersed phase (oil) was more viscous than the continuous phase (water + surfactant). We analyzed the effect of the flow rate of both phases and the viscosity of the dispersed phase on the size of the droplets formed.

With the lower viscosity oil, the drop size is not a function of the continuous phase flow rate but only a function of the flow rate ratio Q_d/Q_c . At low flow rate ratio, the drops are formed by what is called the squeezing mechanism and its size is almost constant. As the flow rate ratio rises, the drops becomes larger and the breakup of the dispersed phase occurs downstream of the secondary channel. This is what is referred to as dripping mechanism in the literature. With the higher viscosity oil, the drop size is a strong function of the continuous phase flow rate. Because of the high

viscosity, the drops resist strongly the deformation and long drops are formed at high oil flow rates, in what is called the jetting mechanism.

In summary, we observed that drops can be formed by three different mechanisms, as discussed in the literature: squeezing, dripping and jetting. However, unlike the results presented in the literature, the transition between different regimes is not defined simply by the capillary number based on the continuous phase flow rate. Our results show different breakup regimes occurring at the same capillary number, but different dispersed flow rate and viscosity.

The results presented here can help understand emulsion formation in the two-phase flow inside porous media, since flow inside microfluid devices, such as the one studied here, represent a good model of the pore scale flow.

5. ACKNOWLEDGEMENTS

D. García was supported by CAPES agency and PUC-Rio through a scholarship. This research was funded by PETROBRAS.

6. REFERENCES

- Christopher, G.F., Noharuddin, N.N., Taylor, J.A., Anna S.L., 2008, "Experimental observations of the squeezing-to-dripping transition in T-shaped microfluidic junctions". *J. Am. Phys. Soc.* 036317, 1–12.
- De Menech, M., Garstecki, P., Jousse, F., Stone, H.A., 2008, "Transition from squeezing to dripping in a microfluidic T-shaped junction". *J. Fluid Mech.* 595, 141–161.
- Fu, T., Ma, Y., Funfschilling, D., Zhu, C., Li, H.Z., 2010, "Squeezing-to-dripping transition for bubble formation in a microfluidic T-junction". *Chem. Engng. Sci.* 65, 3739–3748.
- Garstecki, P., Fuerstman, M.J., Stone, H.A., Whitesides, G.M., 2006, "Formation of droplets and bubbles in a microfluidic T-junction: scaling and mechanism of break-up". *Lab Chip* 6, 437–446.
- Gunther, A., Kahn, S.A., Thalmann, M., Trachsel, F., Jensen, K.F., 2004, "Transport and reaction in microscale segmented gas–liquid". *Lab Chip* 4, 278–286.
- Kokal, S., 2005, "Crude-oil emulsions: a state-of-the-art review". *SPE Prod Facilities.* 20, 5–13.
- Nisisako, T., Okushima, S., Torii, T., 2005, "Controlled formulation of monodisperse double emulsions in a multiple-phase microfluidic system". *Soft Matter*, 1, 23–27.
- Raïkar, N.B., Bhatia, S.R., Malone, M.F., Henson, M.A., 2009, "Experimental studies and population balance equation models for breakage prediction of emulsion drop size distributions". *Chem. Engng. Sci.* 64, 2433–2447.
- Thorsen, T., Roberts, R.W., Arnold, F.H., Quake, S.R., 2001, "Dynamic pattern formation in a vesicle-generating microfluidic device". *Phys. Rev. Lett.* 86, 4163–4166.
- Tice, J.D., Lyon, A.D., Ismagilov, R.F., 2004, "Effects of viscosity on droplet formation and mixing in microfluidic channels". *An. Chim. Acta* 507, 73–77.
- Umbanhowar, P.B., Prasad, V., Weitz, D.A., 2000, "Monodisperse emulsion generation via drop break off in a coflowing stream". *Langmuir* 16, 347–351.
- Xu, J.H., Li, S.W., Tan, J., Luo, G.S., 2008, "Correlations of droplet formation in T-junction microfluidic devices: from squeezing to dripping". *Micr. Nano.* 5, 711–717.
- Zheng, B., Tice, J.D., Ismagilov, R.F., 2004, "Formation of arrayed droplets by soft lithography and two-phase fluid flow, and application in protein crystallization". *Adv. Mater.*, 2004, 16, 1365–1368.

7. RESPONSIBILITY NOTICE

The authors are the only responsible for the printed material included in this paper.